Title

Molecular chaperone TRAP1 regulates a metabolic switch between mitochondrial respiration and aerobic glycolysis.

Journal

Proceedings of the National Academy of Sciences of USA, 110(17)

Authors

Yoshida, Soichiro
Tsutsumi, Shinji
Muhlebach, Guillaume
et al.

Publication Date

2013-04-23

DOI

10.1073/pnas.1220659110

Peer reviewed

Molecular chaperone TRAP1 regulates a metabolic switch between mitochondrial respiration and aerobic glycolysis

Soichiro Yoshida[a,1], Shinji Tsutsumi[a,1], Guillaume Muhlebach[b,1], Carole Sourbier[a], Min-Jung Lee[c], Sunmin Lee[c], Evangelia Vartholomaiou[b], Manabu Tatokoro[a,d], Kristin Beebe[a], Naoto Miyajima[a], Robert P. Mohney[e], Yang Chen[e], Hisashi Hasumi[a], Wanping Xu[a], Hiroshi Fukushima[d], Ken Nakamura[f], Fumitaka Koga[d], Kazunori Kihara[d], Jane Trepel[c], Didier Picard[b], and Leonard Neckers[a,2]

[a]Urologic Oncology Branch and [c]Medical Oncology Branch, Center for Cancer Research, National Cancer Institute, Bethesda, MD 20892; [b]Department of Cell Biology, University of Geneva, CH-1211 Geneva 4, Switzerland; [e]Metabolon, Durham, NC 27560; [d]Department of Urology, Tokyo Medical and Dental University, Tokyo 113-8510, Japan; and [f]Gladstone Institute of Neurological Disease, University of California at San Francisco School of Medicine, San Francisco, CA 94158

Edited* by Sue Wickner, National Cancer Institute, National Institutes of Health, Bethesda, MD, and approved March 12, 2013 (received for review November 27, 2012)

TRAP1 (TNF receptor-associated protein), a member of the HSP90 chaperone family, is found predominantly in mitochondria. TRAP1 is broadly considered to be an anticancer molecular target. However, current inhibitors cannot distinguish between HSP90 and TRAP1, making their utility as probes of TRAP1-specific function questionable. Some cancers express less TRAP1 than do their normal tissue counterparts, suggesting that TRAP1 function in mitochondria of normal and transformed cells is more complex than previously appreciated. We have used TRAP1-null cells and transient TRAP1 silencing/overexpression to show that TRAP1 regulates a metabolic switch between oxidative phosphorylation and aerobic glycolysis in immortalized mouse fibroblasts and in human tumor cells. TRAP1-deficiency promotes an increase in mitochondrial respiration and fatty acid oxidation, and in cellular accumulation of tricarboxylic acid cycle intermediates, ATP and reactive oxygen species. At the same time, glucose metabolism is suppressed. TRAP1-deficient cells also display strikingly enhanced invasiveness. TRAP1 interaction with and regulation of mitochondrial c-Src provide a mechanistic basis for these phenotypes. Taken together with the observation that TRAP1 expression is inversely correlated with tumor grade in several cancers, these data suggest that, in some settings, this mitochondrial molecular chaperone may act as a tumor suppressor.

Molecular chaperones help to maintain cellular homeostasis. The heat-shock protein 90 (HSP90) family of molecular chaperones is highly conserved from bacteria to mammals. HSP90 itself is an essential molecular chaperone found in the cytoplasm and nucleus of all eukaryotic cells (1, 2). In multicellular eukaryotes, the HSP90 family includes the mitochondrial chaperone TRAP1 (TNF receptor-associated protein), which shares 50% sequence similarity with HSP90. Although TRAP1 binds and hydrolyzes ATP in an analogous manner to HSP90 (3), its cellular function is less well understood. Thus, although many HSP90-dependent proteins ("clients") and interacting cochaperones have been described (www.picard.ch/downloads/Hsp90interactors.pdf), the validated list of TRAP1-dependent clients is quite small and TRAP1-interacting cochaperones, if they exist, have yet to be identified (4).

Several studies have suggested that TRAP1 plays a cytoprotective role by buffering reactive oxygen species (ROS)-mediated oxidative stress (5, 6), and others have reported that TRAP1 overexpression attenuates ROS production (7). The antioxidant properties of TRAP1, together with its reported ability to regulate opening of the mitochondrial permeability transition pore (8, 9), may contribute to its antiapoptotic activity (4). For these reasons, TRAP1 has been proposed as an anticancer molecular target, and first-generation inhibitors have shown some anticancer activity in preclinical models (10). However, these inhibitors do not distinguish between HSP90 and TRAP1 (11), and TRAP1 expression in cancer is variable but HSP90 comprises as much as 5% of a cancer cell's protein complement (12). Indeed, some cancers express less TRAP1 than do their normal tissue counterparts (13). Thus, the functions of TRAP1 in mitochondria of normal and transformed cells are likely more complex than previously appreciated and, in the absence of TRAP1-specific inhibitors, other approaches are necessary to investigate TRAP1-specific cellular effects.

In this study, we have explored the metabolic and phenotypic consequences of TRAP1 gene disruption/knockdown and overexpression in fibroblast cell lines established from adult WT and TRAP1-null mice, and in human tumor cells transiently transfected with either TRAP1-specific siRNA or TRAP1 expression plasmids. We show that loss of TRAP1 results in increased mitochondrial oxygen consumption, elevated levels of tricarboxylic acid (TCA) cycle intermediates, and increased steady-state ATP and ROS levels, with concomitant suppression of aerobic glycolysis, but overexpression of TRAP1 has the opposite effect. Absence of c-Src expression abrogates the ability of TRAP1 to modulate mitochondrial respiration and ATP level, and TRAP1 and c-Src colocalize and interact within mitochondria. Our data

Significance

TNF receptor-associated protein (TRAP1) is found predominantly in mitochondria. A possible direct impact of TRAP1 on mitochondrial metabolism remains unexplored. We used TRAP1-null cells and transient TRAP1 silencing/overexpression to show that TRAP1 regulates a metabolic switch between oxidative phosphorylation and aerobic glycolysis in immortalized mouse fibroblasts and in human tumor cells. TRAP1 deficiency promotes increased mitochondrial respiration, fatty acid oxidation, tricarboxylic acid cycle intermediates, ATP and reactive oxygen species, while concomitantly suppressing glucose metabolism. TRAP1 deficiency also results in strikingly enhanced cell motility and invasiveness. TRAP1 interaction with and regulation of mitochondrial c-Src provide a mechanistic basis for these phenotypes.

Author contributions: S.Y., K.N., F.K., K.K., J.T., D.P., and L.N. designed research; S.Y., S.T., G.M., C.S., M.-J.L., S.L., E.V., M.T., K.B., N.M., R.P.M., Y.C., H.H., W.X., H.F., K.N., and F.K. performed research; G.M., C.S., and E.V. contributed new reagents/analytic tools; S.Y., S.T., G.M., C.S., M.-J.L., S.L., E.V., M.T., K.B., N.M., R.P.M., Y.C., H.H., H.F., K.N., F.K., K.K., J.T., D.P., and L.N. analyzed data; and S.Y., D.P., and L.N. wrote the paper.

The authors declare no conflict of interest.

*This Direct Submission article had a prearranged editor.

[1]S.Y., S.T., and G.M. contributed equally to this work.

[2]To whom correspondence should be addressed. E-mail: neckersl@mail.nih.gov.

This article contains supporting information online at www.pnas.org/lookup/suppl/doi:10.1073/pnas.1220659110/-/DCSupplemental.

are thus consistent with a model in which TRAP1 regulates the previously reported ability of mitochondrial c-Src to stimulate oxidative phosphorylation (14, 15). Reduced/absent TRAP1 expression also correlates with increased cell motility/invasiveness that is sensitive to c-Src inhibition and ROS buffering strategies. These findings highlight a previously unrecognized physiological role for TRAP1 in regulating the metabolic balance between oxidative phosphorylation and aerobic glycolysis, and they support an indirect role for TRAP1 in suppressing c-Src– and ROS-dependent cell invasion.

Results

TRAP1 Deficiency Is Associated with Increased Mitochondrial Respiration and Decreased Glycolysis. We established fibroblast cell lines (termed MAFs, murine adult fibroblasts) from adult TRAP1$^{-/-}$ (null, hereafter referred to as KO) and WT mice to explore the metabolic consequences of TRAP1 knockout. We confirmed the absence of TRAP1 protein expression in two independently derived MAF cell lines (Fig. 1*A*). Because TRAP1 is primarily localized to mitochondria, we first asked whether TRAP1 knockout affects mitochondrial mass. Using flow cytometric analysis of MitoTracker Green-labeled cells, we saw no increase in signal in KO cells compared with WT (Fig. S1*A*). In addition, assessment of mitochondrial membrane potential revealed no difference between WT and TRAP1 KO MAFs (Fig. S1*B*).

To assess the possible impact of TRAP1 loss on mitochondrial function, we measured mitochondrial respiration by determining the cellular oxygen consumption rate (OCR) in WT and TRAP1 KO cells using an extracellular flux analyzer. KO cells displayed a higher basal OCR and a significantly higher maximum respiratory capacity [e.g., OCR determined after treatment with the ATP synthase inhibitor oligomycin and the chemical uncoupler carbonyl cyanide-p-trifluoromethoxyphenylhydrazone (FCCP); see *Methods*)] compared with WT, and this was accompanied by significantly decreased glycolysis (extracellular acidification rate, ECAR, is an indicator of glycolysis; see *Methods*) (Fig. 1*B*). Importantly, oxygen consumption in KO cells was reduced to the level of WT upon stable reintroduction of exogenous TRAP1, supporting the likelihood that the metabolic disparity between TRAP1 WT and KO cells is TRAP1-dependent (Fig. S1*C*). To confirm these data from intact cells, we assessed the basal OCR of mitochondrial preparations isolated from cells grown in DMEM (containing 4.5 g/L glucose and Glutamax; see *Methods*). After normalization to total mitochondrial protein, the OCR of mitochondria prepared from KO cells was significantly increased compared with the OCR of mitochondria prepared from WT cells (Fig. 1*C*). These data support the hypothesis that the mitochondria of TRAP1 KO cells consume a significantly greater amount of oxygen compared with WT, suggesting a preference for oxidative phosphorylation over aerobic glycolysis.

In agreement with this possibility, metabolomic analysis of WT and TRAP1 KO cell lines revealed marked reduction in the steady-state levels of several glycolytic metabolites, but the levels of several TCA cycle metabolites (e.g., α-ketoglutarate and citrate) were increased (Fig. 1*D*). Also increased was the anaplerotic substrate propionylcarnitine, a metabolic precursor of propionyl CoA, which in turn is converted to oxaloacetate to replenish TCA cycle intermediates (16–19). Fatty acid oxidation is also significantly increased in TRAP1 KO MAFs compared with WT cells (Fig. 1*E*), as is the NAD^+/NADH ratio (2.5-fold higher in TRAP1 KO vs. WT cells, $P = 0.02$), consistent with increased oxygen consumption and suggesting increased metabolic flux through the TCA cycle of TRAP1 KO cells that is independent of glucose metabolism (Fig. 1*D* and Fig. S1*D*).

ATP Levels and Mitochondrial Complex IV Activity Are Elevated in TRAP1-Deficient Cells. Because mitochondrial respiration is a more efficient generator of ATP than is glycolysis, we asked whether TRAP1 KO cells produce more ATP compared with WT cells (Fig. 1*F*). Indeed, steady-state ATP levels in both TRAP1 KO cell lines were significantly higher than in either WT cell line. Metabolomic analysis independently confirmed the increased steady-state ATP concentration in TRAP1 KO cells (Fig. 1*D*). To determine whether changes in ATP production in the KO cells are a consequence of TRAP1 deficiency, we reexpressed TRAP1 (GFP-tagged) in KO cells. The mean ATP level of the transfected population (estimated transfection efficiency of 60–70% based on GFP expression) was significantly reduced compared with that of empty (GFP) plasmid-transfected TRAP1 KO cells (Fig. 1*G*).

Mitochondrial complex IV (cytochrome *c* oxidase) is the last enzyme in the respiratory electron transport chain, converting molecular oxygen to water while providing the electrochemical potential used by ATP synthase (complex V) to produce ATP. We examined whether complex IV enzymatic activity was increased in TRAP1 KO cells compared with WT, and found that both independently derived TRAP1 KO MAF cell lines displayed elevated complex IV activity compared with WT cells (Fig. S1*E*). Based on the slopes of the absorbance curves (WT = 0.373, KO1 = 0.906, KO2 = 0.657), complex IV activity is increased approximately twofold in TRAP1 KO cells compared with WT. These data are consistent with the hypothesis that loss of TRAP1 expression deregulates mitochondrial respiration and ATP production.

We extended these results by investigating the impact of transient TRAP1 deficiency or overexpression on mitochondrial respiration and ATP levels in human tumor cells (HeLa and HCT116 cell lines). Using HeLa cells, we verified the predominant mitochondrial localization of transiently expressed TRAP1-Flag and TRAP1-GFP proteins (Fig. S1*F*) and the efficiency of siRNA-mediated silencing of endogenous TRAP1 (Fig. S1*G*). In agreement with the data we obtained from TRAP1 WT and KO MAFs, transient TRAP1 knockdown in HeLa cells resulted in a nearly twofold increase in the OCR of isolated mitochondria (Fig. 1*H*). TRAP1 silencing also significantly increased the OCR and steady-state ATP level in HCT116 cells (Fig. S1 *H–J*). Also in accord with our data from mouse fibroblasts, TRAP1 overexpression significantly reduced the OCR and cellular ATP level of HeLa cell mitochondria (Fig. 1 *I* and *J*) and the OCR in HCT116 mitochondria (Fig. S1*K*).

How does TRAP1 affect the balance between mitochondrial respiration and aerobic glycolysis? One of the key regulatory steps in commitment to glycolysis is conversion of fructose 6-phosphate to fructose 1,6-bisphosphate by phosphofructokinase (PFK), because this reaction is irreversible. High cellular ATP levels allosterically inhibit PFK activity (20). PFK is also inhibited by abundant citrate, another indicator of a cell's high energy state (21, 22). Because TRAP1 deficiency causes a high energy state (elevated ATP and citrate), we queried whether TRAP1 KO MAFs contained reduced levels of fructose 1,6-bisphosphate. Indeed, fructose 1,6-bisphosphate levels were reduced by more than 90% in TRAP1 KO fibroblasts compared with WT cells (Fig. 1*K*). However, when mitochondrial ATP synthase was poisoned with oligomycin for 30 min, long enough for ATP levels to decline, both WT and TRAP1 KO cells were equally capable of producing ATP by glycolysis (Fig. 1 *L* and *M*, respectively), supporting the hypothesis that the reduced glycolysis characteristic of TRAP1-deficient cells is an indirect and reversible consequence of these cells' high energy state caused by deregulated mitochondrial respiration.

ROS Are Elevated in TRAP1-Deficient Cells. Because the mitochondrial electron transport chain is a significant source of cellular ROS, we determined whether the increased mitochondrial respiration occurring as a consequence of TRAP1 deficiency leads to elevated ROS. In agreement with previous reports (5–7), we observed a strong inverse correlation between oxidation of

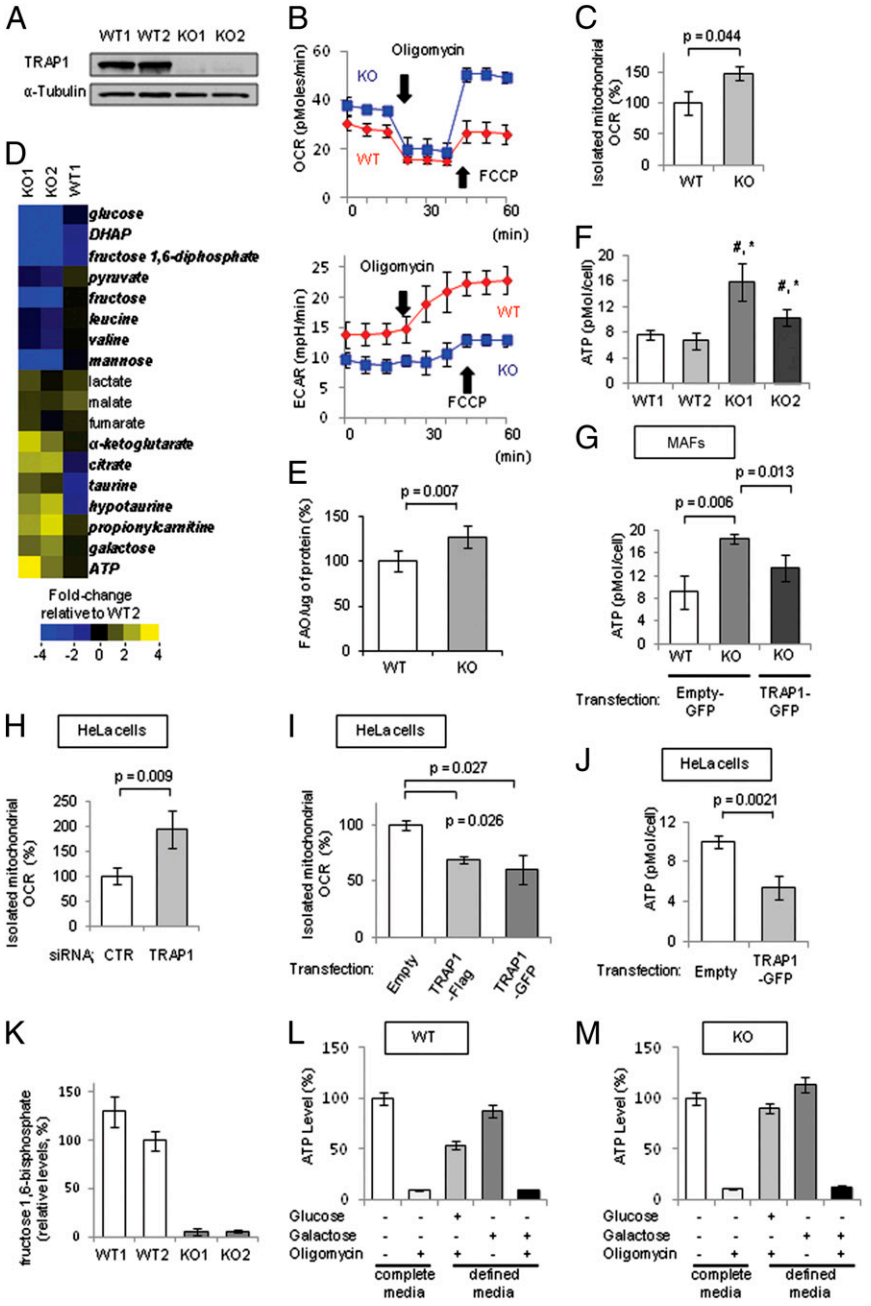

Fig. 1. TRAP1 negatively regulates mitochondrial respiration and ATP level. (*A*) TRAP1 protein expression of WT and TRAP1 KO MAFs was analyzed by Western blot; α-tubulin was used as loading control. (*B*) OCR and ECAR of WT and TRAP1 KO MAF cells were monitored by using the Seahorse Bioscience Extra Cellular Flux Analyzer in real time. Cells were treated sequentially with oligomycin (1 μM) and FCCP (0.3 μM). OCR is an indicator of mitochondrial respiration and ECAR is predominately a measure of glycolytic flux (mean ± SD, $n = 3$). (*C*) Basal OCR of isolated mitochondria of WT and TRAP1 KO cells was assessed using the Seahorse Bioscience Flux Analyzer (mean ± SD, $n = 3$ per group). (*D*) Metabolomic analysis of compounds related to glycolysis and mitochondrial respiration, and ATP levels, in WT (two independent clones) and TRAP1 KO (two independent clones) cells. The median value of each metabolite was calculated from six replicates. The fold-change relative to WT2 is indicated by the color of each box (see also Fig. S1*E*). Metabolite names shown in italic bold font indicate significantly altered metabolites between WT and TRAP1 KO cells ($P < 0.05$). (*E*) Fatty acid oxidation in WT and TRAP1 KO cells was assessed using the Seahorse Bioscience Flux Analyzer (mean ± SD, $n = 5$ per group). (*F*) ATP levels were assessed in two independent WT and TRAP1 KO clones (mean ± SD, $n = 3$ for each clone; $^{\#}P < 0.01$ compared with WT1, $^{*}P < 0.01$ compared with WT2). Data were normalized for cell number. (*G*) ATP level in KO MAFs was assessed after transduction with TRAP1-GFP or empty-GFP plasmid (mean ± SD, $n = 3$ per group). ATP level in WT MAFs transfected with empty-GFP plasmid is shown for comparison. (*H*) Isolated mitochondrial OCR of HeLa cells 72 h after transfection with control (CTR) or TRAP1 siRNA was assessed using the Seahorse Bioscience Flux Analyzer (mean ± SD, $n = 3$ per group). (*I*) OCR of isolated mitochondria prepared from HeLa cells 72 h after transfection with TRAP1-Flag or TRAP1-GFP plasmids was assessed using the Seahorse Bioscience Flux Analyzer (mean ± SD, $n = 3$ per group). (*J*) ATP levels were assessed in HeLa cells 24 h after transfection with TRAP1-GFP or empty plasmid. Transfection did not affect cell viability (mean ± SD, $n = 3$ per group). (*K*) Fructose 1,6-bisphosphate levels were determined in two WT and two TRAP1 KO fibroblast clones by metabolomic analysis (*Methods*). Values are normalized by cell number. Mean ± SD is shown; for each group, $n = 6$. (*L*) TRAP1 WT MAFs (5,000 cells per well) were seeded in 96-well plates in complete medium (DMEM with 10% FBS and Glutamax). Twenty-four hours later, medium was aspirated, cells were washed twice in PBS, and either complete or defined medium (lacking glutamine, pyruvate, galactose, and glucose) was added. Galactose (10 mM) or glucose (10 mM) were added to defined media where shown. After 3 h, oligomycin (10 μg/mL, final) was added to inactivate mitochondrial ATP synthase and ATP levels were measured after 30 min. Data were normalized to cell number. Mean ± SD is shown; for each group, $n = 6$. (*M*) TRAP1 KO MAFs were treated and analyzed as in *L*.

CM-H_2DCFDA, an indicator of total cellular ROS, and TRAP1 expression in both mouse fibroblasts and HCT116 cells (Fig. 2 *A*–*C*). Furthermore, mitochondrial superoxide assessed with MitoSOX Red reagent was also significantly increased in HCT116 cells upon TRAP1 silencing (Fig. 2 *D* and *E*). Finally, lipid peroxidation was significantly increased in TRAP1 KO MAFs compared with WT MAFs (Fig. 2*F*), consistent with the likelihood that TRAP1 KO cells are constitutively exposed to elevated oxidative stress. Interestingly, taurine, hypotaurine, and propionylcarnitine have all been reported to protect cells from oxidative stress (23–29). Thus, the elevated levels of these metabolites in TRAP1 KO cells (Fig. 1*D*) may reflect up-regulation, albeit limited, of alternative buffering mechanisms to compensate for loss of TRAP1 expression.

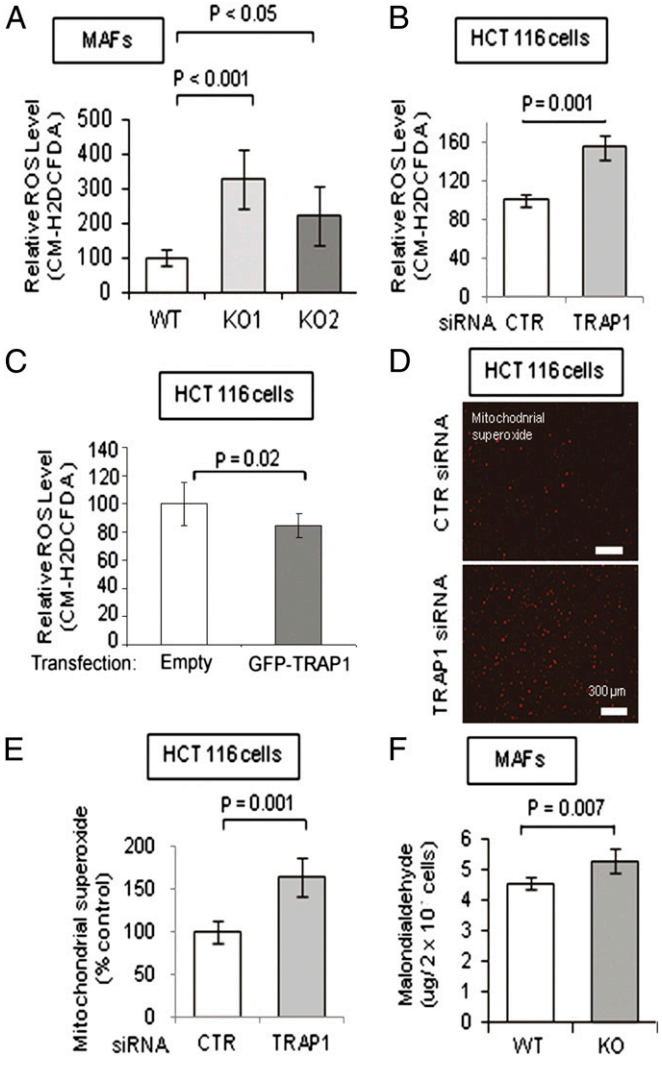

Fig. 2. TRAP1 expression inhibits ROS production. (*A*) Steady-state ROS level was measured with CM-H_2DCFDA in WT or TRAP1 KO MAF cells (mean ± SD). (*B*) ROS level was measured with CM-H_2DCFDA in HCT116 cells 72 h after transfection with control (CTR) or TRAP1 siRNA (mean ± SD). (*C*) ROS level was measured as in *B* in HCT116 cells 72 h after transfection with empty plasmid or GFP-TRAP1 plasmid (mean ± SD). (*D*) Representative images of HCT116 cells stained with MitoSOX RED to detect mitochondrial superoxide 72 h after transfection with TRAP1 or control (CTR) siRNA. (*E*) Quantification of the extent of mitochondrial superoxide detected with MitoSOX RED in HCT116 cells 72 h after transfection with control (CTR) or TRAP1 siRNA (mean ± SD, $n = 3$ per group). (*F*) Lipid peroxidation in WT and TRAP1 KO MAFs. The end product of lipid peroxidation, malondialdhyde (MDA), was measured; data are expressed as mean ± SD ($n = 5$ per group).

TRAP1 Interacts with Mitochondrial c-Src and Suppresses Its Activity. How does TRAP1 regulate mitochondrial respiration? Because TRAP1 is a member of the HSP90 chaperone family, whose clientele is rich in cytosolic and nuclear kinases (2) (www.picard.ch/downloads/Hsp90interactors.pdf), we hypothesized that the impact of TRAP1 on mitochondrial respiration may be mediated, at least in part, by interaction with/regulation of one or more mitochondrial kinases. Unexpectedly, we found TRAP1 to be tyrosine phosphorylated (Fig. 3*A*, *Left*), which caused us to examine c-Src, a kinase reported to be present in mitochondria (14, 15, 30–33). We probed TRAP1 immunoprecipitates for c-Src association and we identified c-Src as a TRAP1-interacting protein in HCT116 cells (Fig. 3*A*, *Center*) and in HeLa cells (Fig. 3*G*). Using reciprocal immunoprecipitations, we validated the interaction between endogenous c-Src and endogenous TRAP1 in HCT116 cells (Fig. 3*B*). In agreement with previous reports, we identified both TRAP1 and c-Src in mitochondrial preparations whose purity was confirmed by reciprocal blotting for VDAC (voltage-dependent anion channel, a mitochondrial marker) and β-actin (a cytosolic protein) (Fig. 3*C*). Analysis of subfractionated HeLa cell mitochondrial preparations demonstrated TRAP1 localization to the inner mitochondrial membrane and mitochondrial matrix (Fig. S2*A*), the same location described for mitochondrial c-Src (14). We confirmed colocalization of c-Src and TRAP1 in isolated HeLa cell mitochondria by demonstrating their similar sensitivity to proteinase K (Fig. S2*B*). Similar to HSP60, which is localized to the mitochondrial matrix (34), full proteinase K sensitivity of both TRAP1 and c-Src requires detergent permeabilization of isolated mitochondria (Table S1).

To query the functional significance of the c-Src–TRAP1 interaction, we measured the intensity of mitochondrial c-Src Tyr-416 phosphorylation, an indicator of c-Src activation state, in WT and TRAP1 KO fibroblasts. We observed that c-Src Tyr-416 phosphorylation was markedly increased in TRAP1 KO mitochondria compared with mitochondria of WT cells, although mitochondrial c-Src levels were equivalent (Fig. 3*D*). Importantly, Tyr-416 phosphorylation of cytosolic c-Src in TRAP1 KO cells was negligible, supporting the specificity of the impact of TRAP1 expression on mitochondrial c-Src activation. Mitochondrial c-Src Tyr-416 phosphorylation was significantly reduced following TRAP1 overexpression in HCT116 cells and in TRAP1 KO fibroblasts (Fig. 3 *E* and *F*, and Fig. S2*C*).

We next investigated whether c-Src phosphorylation status affected its interaction with TRAP1. After treating TRAP1 and c-Src cotransfected cells with the c-Src inhibitor dasatinib, we observed that mitochondrial c-Src autophosphorylation was abolished (Fig. S2*D*). However, immunoprecipitation of either c-Src or TRAP1 from HCT116 and HeLa cells revealed that interaction of the two proteins was markedly enhanced following c-Src inactivation, suggesting that TRAP1 preferentially binds the inactive form of c-Src (Fig. 3G and Fig. S2*E*). Because c-Src overexpression induced dasatinib-sensitive TRAP1 tyrosine phosphorylation (Fig. 3*G*), we speculate that c-Src-mediated TRAP1 phosphorylation disrupts TRAP1/c-Src interaction and TRAP1 binding to c-Src inhibits its kinase activity.

TRAP1 and Mitochondrial c-Src Have Opposing Effects on Mitochondrial Respiration. Based on these data and on previous reports that mitochondrial c-Src stimulates complex IV activity and enhances oxidative phosphorylation (14, 15), we speculated that the effect of TRAP1 on mitochondrial respiration may depend on its regulation of mitochondrial c-Src. To investigate this possibility, we confirmed that c-Src overexpression significantly increased the OCR of isolated HeLa cell mitochondria, but

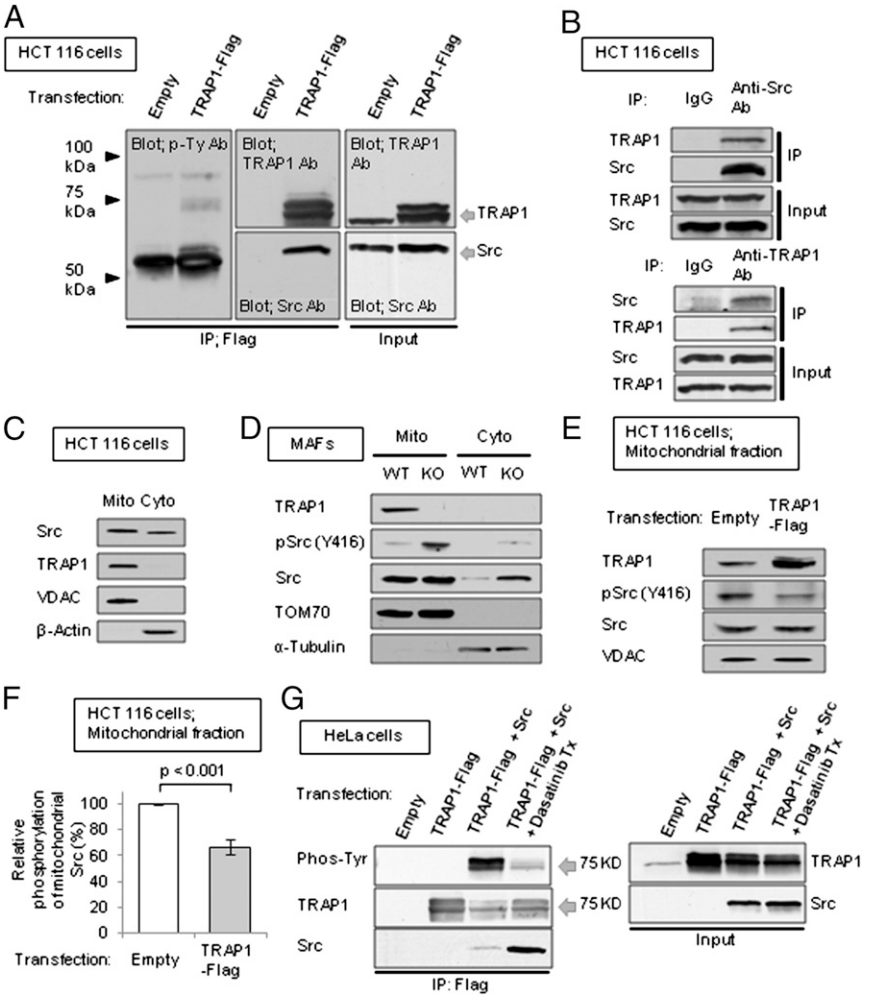

Fig. 3. TRAP1 interacts with mitochondrial c-Src and regulates its activity. (*A*) TRAP1-Flag was immunoprecipitated (with anti-Flag antibody) from HCT 116 cells transfected 24 h previously with TRAP1-Flag. Blots were probed with antibodies directed toward pan-phosphotyrosine, TRAP1, or c-Src. Lysate inputs are shown for comparison. (*B*) HCT116 cell lysates were immunoprecipited with anti-TRAP1 or anti-Src antibody and blotted with the reciprocal antibody. (*C*) HCT116 cells were fractionated into mitochondria or cytosolic extracts and analyzed by Western blot for c-Src, TRAP1, VDAC (marker of mitochondrial fraction), and β-actin (marker of cytosolic fraction). (*D*) WT and TRAP1 KO MAF cells were fractionated into mitochondrial or cytosolic fractions and fractions were blotted for TRAP1, phospho-Src and total c-Src. TOM70 and α-tubulin were used to check the purity of mitochondrial and cytosolic fractions, respectively. (*E*) Mitochondrial fraction of HCT116 cells transfected with empty or TRAP1-Flag plasmid was prepared and TRAP1, phospho-Src and total c-Src proteins were detected by Western blot. VDAC was used as loading control. (*F*) Relative phosphorylation of mitochondrial c-Src in HCT116 cells transfected with empty or TRAP1-Flag plasmids was assessed by Western blot and densitometrically quantified (mean ± SD, $n = 3$ per group). (*G*) HeLa cells were cotransfected with either empty or TRAP1-Flag plasmids, and with either empty or c-Src plasmids. TRAP1-Flag was immunoprecipitated, and associated c-Src and tyrosine phosphorylated TRAP1 were detected by Western blotting. Before lysis, some cells were treated with 50 nM dasatinib for 3 h.

simultaneous overexpression of TRAP1 partially reversed this effect (Fig. 4*A*). To confirm the importance of mitochondrial c-Src in this process, we assessed the OCR in HEK293 cells transiently transfected with various mitochondrially targeted c-Src constructs (WT, constitutively active, kinase-dead) (15), in the presence or absence of cotransfected TRAP1 (Fig. S3 *A* and *B*). Both WT and constitutively active mitochondrially targeted c-Src, but not kinase-dead c-Src, increased OCR in HEK293 compared with transfection with empty plasmid. Importantly, cotransfection of TRAP1 with either WT or constitutively active mitochondrially targeted c-Src completely reversed the increase in OCR. c-Src overexpression also increased the steady-state ATP level in HeLa cells (Fig. S3*C*). Consistent with these data, both the OCR and ATP level of stably v-Src–transformed 3T3 cells was significantly greater than that of nontransformed 3T3 (Fig. S3 *D* and *E*). Next, we observed that the c-Src inhibitor dasatinib caused a significant reduction in the OCR of both WT and TRAP1 KO fibroblasts (Fig. 4*B*). Taken together, these data are consistent with the hypothesis that mitochondrial c-Src and TRAP1 exert opposing effects on cellular respiration and that the increased OCR seen in TRAP1 KO cells is at least partially a consequence of deregulated mitochondrial c-Src.

To provide further support for this hypothesis, we evaluated the impact of decreased TRAP1 expression on ATP level and mitochondrial OCR in Src family kinase-deficient ($Src^{-/-}$ $Fyn^{-/-}$ $Yes^{-/-}$, SFY) murine embryo fibroblasts (MEFs), and in c-Src–restored (SFY-Src) MEFs. We used siRNA to efficiently silence TRAP1 expression in both SFY and SFY-Src MEFs (Fig. S3 *F* and *G*). In contrast to our previous data, TRAP1 knockdown failed to increase either OCR or ATP level in parental SFY cells (Fig. 4 *C* and *D*). However, both OCR and ATP level in SFY-Src cells were significantly increased upon TRAP1 knockdown (Fig. 4 *E* and *F*). These findings strongly suggest that the impact of TRAP1 on mitochondrial respiration requires and is mediated by modulation of mitochondrial c-Src.

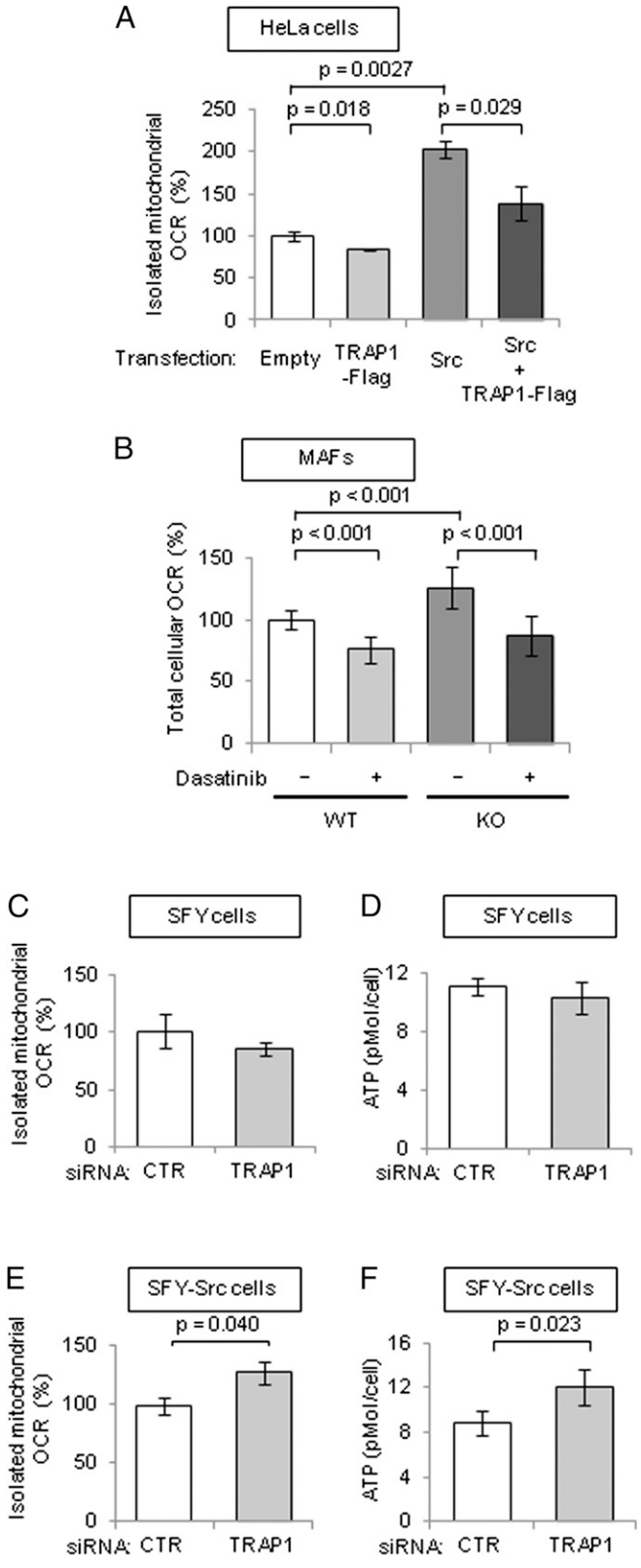

Fig. 4. TRAP1 suppression of mitochondrial respiration requires c-Src expression. (*A*) Isolated mitochondrial OCR of HeLa cells cotransfected with either empty or TRAP1-Flag plasmids, and with either empty or c-Src plasmids (mean ± SD, *n* = 3 per group). (*B*) WT and TRAP1 KO MAF cells were treated with 100 nM dasatinib or DMSO for 24 h and total cellular OCR was evaluated (mean ± SD, *n* = 3 per group). (*C–F*) Isolated mitochondrial OCR (*C* and *E*) and ATP levels (*D* and *F*) were assessed in SFY (*C* and *D*) or SFY-Src (*E* and *F*) cells 72 h after transfection with control (CTR) or Trap1 siRNA (mean ± SD, *n* = 3 per group).

TRAP1 Deficiency Potentiates Cell Invasion. Because elevated ROS are reported to stimulate cell invasion (35, 36), we examined whether TRAP1 expression affected this phenotype. Unlike WT cells, TRAP1 KO MAFs displayed a strikingly enhanced ability to invade through Matrigel-coated membranes, and this activity was sensitive to both the c-Src inhibitor dasatinib and the ROS scavenging agent ascorbic acid (Fig. 5*A*). Importantly, ascorbic acid dose-dependently reduced, and the oxidizing agent hydrogen peroxide dose-dependently increased c-Src autophosphorylation (Fig. S4 *A* and *B*), suggesting that the elevated ROS level in TRAP1-deficient cells may contribute to c-Src activation and enhanced cell invasion. TRAP1 silencing in several cell lines, including HCT116, HEK293, and Caki-1, similarly resulted in increased cell invasion (Fig. 5 *B*, *F*, and *G*), but TRAP1 overexpression in HeLa cells significantly decreased this activity (Fig. 5 *C–E*).

TRAP1 Expression Correlates Inversely with Tumor Stage in Cervical, Bladder and Clear Cell Renal Cell Cancer. Although TRAP1 is reported to be up-regulated in some cancers, its expression is diminished in others (8, 37–39). The impact of reduced TRAP1 expression on in vitro cell invasion raises the possibility that certain more aggressive, metastatic, or late-stage cancers may express less TRAP1 than less advanced tumors. Using meta-analysis of mRNA expression profiles available in publicly accessible databases (*Methods*), we confirmed that TRAP1 expression displays a significant inverse correlation with tumor stage in cervical and bladder cancer (Fig. S5 *A* and *B*). Immunohistochemical analysis of TRAP1 protein expression in normal bladder urothelium and bladder cancer was consistent with these findings (Fig. S5*C*). Furthermore, comparison of TRAP1 protein expression in normal kidney, normal liver, and several clear cell renal cell cancer specimens also demonstrated greater immunoreactivity in normal tissue compared with adjacent tumor (Fig. S5*D*), and evaluation of the intensity of TRAP1 immunoreactivity in localized vs. advanced clear cell renal cell carcinoma specimens (12 cases each) revealed a significant inverse correlation with tumor stage (Table 1).

Discussion

Since Toft and colleagues first cloned TRAP1 in 2000 (40), detailed analysis of the function of this mitochondria-localized molecular chaperone has remained incomplete. Some studies have reported abundant expression of TRAP1 in various cancer tissues but not in normal tissues, and these investigators have suggested that TRAP1 contributes to oncogenesis (41, 42). However, others have found the expression of TRAP1 in both normal and cancer tissues to be more variable (13, 39). Using data from publically available gene-expression databases, as well as archived tumor tissues, we have demonstrated here an inverse correlation between TRAP1 expression and tumor stage in cervical, bladder, and clear cell renal cell carcinoma. Intriguingly, cervical carcinoma is among those cancers whose predominant energy metabolism is via oxidative phosphorylation, not glycolysis (43). Our findings suggest a reevaluation of the assumption that TRAP1 is uniformly pro-oncogenic, and they support a more nuanced role for this mitochondrial chaperone in regulating cellular metabolism and impacting tumorigenesis. In this study, we have identified TRAP1 to be a negative regulator of mitochondrial respiration able to modulate the balance between oxidative phosphorylation and aerobic glycolysis, and we have provided evidence that TRAP1 interaction with, and modulation of the activity of mitochondrial c-Src is essential for this function.

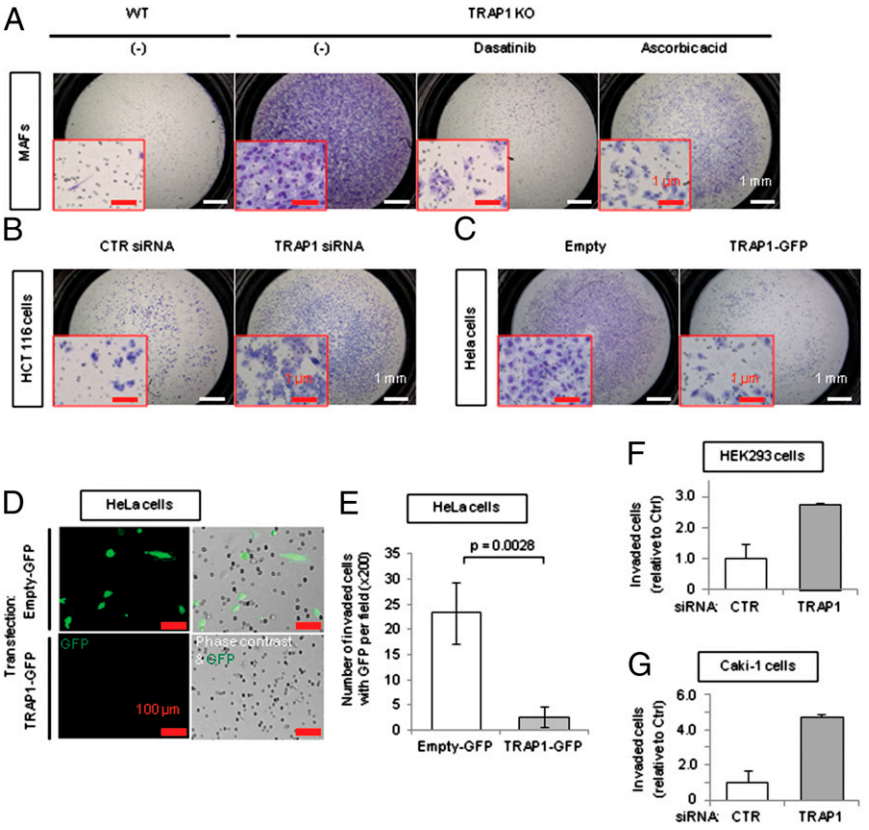

Fig. 5. TRAP1 impact on cell invasion is Src- and ROS-dependent. (*A–C*) Representative images of 24-well Matrigel-coated cell invasion chamber membranes. WT and TRAP1 KO MAF cells were allowed to invade through the membranes for 24 h in the presence or absence of 100 μM ascorbic acid or 100 nM dasatinib (*A*). HCT116 cells transfected with control (CTR) or TRAP1 siRNA (*B*), and HeLa cells transfected with empty-GFP or TRAP1-GFP plasmids (*C*) were allowed to invade through the membranes for 24 h. (*D*) Representative GFP signal and phase contrast pictures of the invaded cells in *C*. (*E*) The number of invaded cells in *D* that were GFP-positive per field (200×) were assessed (mean ± SD, $n = 3$ per group). HEK293 cells (*F*) and Caki-1 cells (*G*) were treated and analyzed as in *B*. Number of invading cells is graphed relative to control (mean ± SD, $n = 3$ per group).

As a consequence of reduced or absent TRAP1 expression mitochondrial respiration is deregulated, establishing a high energy state characterized by elevated α-ketoglutarate, citrate, and ATP. Aerobic glycolysis is suppressed as a byproduct of this altered metabolic landscape, likely because of, in part, allosteric inhibition of the glycolytic enzyme phosphofructokinase. These data are in general agreement with a recent study showing that TRAP1 silencing in a glioblastoma cell line resulted in a variety of metabolic changes suggestive of reduced glycolysis, including reduced lactic acid secretion (44). Suppression of glycolysis concomitant with enhanced fatty acid oxidation and increased steady-state levels of several TCA cycle intermediates, including oxaloacetate, strongly suggest that TRAP1-deficient cells use one or more anaplerotic mechanisms to sustain their mitochondrial metabolism. Intriguingly, a nearly identical metabolic phenotype has been described for castrate-resistant prostate cancer (45), and a recent study suggests that oxidative phosphorylation may play a prominent role in advanced melanoma (46). Although evaluation of TRAP1-specific inhibitors warrants further exploration as a novel approach to cancer therapy, our findings would suggest that TRAP1 inhibition alone is unlikely to be a viable treatment strategy for cancers that use oxidative phosphorylation.

Table 1. Comparison of TRAP1 protein expression in localized and advanced clear cell renal cell carcinoma

TRAP1 staining intensity	–	+/–	+/++
Clear cell renal cell cancer/localized disease ($n = 12$)	1	3	8
Clear cell renal cell cancer/advanced disease ($n = 12$)	10	2	0

For the χ^2 test (comparing localized disease to advanced disease): $P = 0.0004$. TRAP1 protein expression in tumor tissue was assessed by immunocytochemistry (see *Methods*) and is compared with that of normal renal tissue (designated "+"). See also Fig. S5.

Although our data were obtained by manipulating TRAP1 protein expression, the impact of TRAP1 on mitochondrial respiration is mediated, at least in part, by its interaction with, and regulation of mitochondrial c-Src. Miyazaki et al. first reported that c-Src is located within mitochondria and affects energy metabolism by phosphorylating complex IV (14). Later studies confirmed that c-Src is present in the inner mitochondrial membrane/matrix (15). Although the mechanism by which TRAP1 regulates mitochondrial c-Src is not yet clarified, the cytosolic c-Src–HSP90 interaction provides a model to address this question. Cytoplasmic c-Src is a well-studied HSP90 client protein and its interaction with HSP90 is required for Src maturation (47). However, we have shown previously that pharmacological disruption of HSP90 association with mature c-Src induces a transient but distinct increase in c-Src activity (48, 49). Release of enzymatically competent c-Src from HSP90 relieves its auto-inhibition and permits phosphorylation of Tyr-416 in the activation loop. In the present study, we observed a similar increase in mitochondrial c-Src Tyr-416 phosphorylation upon TRAP1 suppression or gene disruption, concomitant with increased mitochondrial respiration and ATP production. Furthermore, TRAP1 interacted more efficiently with the inactive

form of c-Src, while also being a c-Src substrate (directly or indirectly). Thus, we propose that regulated association/dissociation of TRAP1 and c-Src, perhaps via TRAP1 phosphorylation, modulates the activity of mitochondrial c-Src which, in turn, affects the rate of mitochondrial respiration.

A number of studies have reported that TRAP1 protects mitochondria from oxidative stress, and that TRAP1 expression and ROS levels are inversely correlated, although the molecular mechanisms underlying this observation have remained to be elucidated. Based on our data, we propose that the elevated ROS generation characteristic of TRAP1-deficient cells is a consequence of deregulated mitochondrial respiration. ROS play important roles in a variety of signaling pathways. For example, multiple protein tyrosine phosphatases are reversibly inactivated by oxidation, and this in turn affects the activity of cytosolic kinases, including c-Src. Deregulated cytosolic c-Src activity promotes cell motility and invasion (50), and TRAP1 knockout or transient suppression dramatically enhances cell invasiveness, both in mouse fibroblasts and in a variety of human cell lines. Importantly, this phenotype is sensitive to c-Src inhibition and ROS neutralization, supporting a direct link between TRAP1 deficiency, elevated ROS, and c-Src activation in mediating this process. The impact of TRAP1 on cellular bioenergetics may also contribute to this phenotype. Interestingly, a recent study reported that transient TRAP1 silencing in cancer cells was associated with up-regulation of a number of cell motility and metastasis-associated genes, and TRAP1 overexpression was associated with increased expression of genes associated with cell proliferation (13). The indirect transcriptional impact of TRAP1 expression requires further exploration, but taken together with our findings these data reinforce the reciprocal relationship between TRAP1 expression and cell motility/invasion, at both the transcriptional and posttranslational level.

Although glucose metabolism is markedly down-regulated in TRAP1 KO cells, these cells are able to use glycolysis to replenish their ATP stores when mitochondrial ATP synthase is inhibited for a long enough period to significantly affect the cellular ATP level. Recent studies have shown that utilization of alternative carbon sources affects tumor evolution, and the role of oxidative phosphorylation in cancer metabolism has not been fully appreciated (46, 51–54). Furthermore, the ability of normal as well as cancer cells to rapidly adjust their metabolic behavior in response to environmental conditions and cellular requirements is essential to survival and the metabolic requirements of proliferating and nonproliferating cells are distinct, as are the metabolic demands underlying tumor initiation, metastasis, and growth at distant sites (55, 56). For these reasons, optimal growth/survival of all normal and most cancer cells would benefit greatly from the ability to use either mitochondrial respiration or glycolysis as conditions warrant. Identification of the mitochondrial chaperone TRAP1 as a key modulator of this metabolic switch provides unique mechanistic insight into its molecular regulation.

Methods

Cell Culture and Reagents. HCT 116, HeLa, COS-7, SFY, SFY-Src, and NIH 3T3 cells were obtained from the American Type Culture Collection. These cells were cultured as directed by the provider. vSrc-transfected NIH/3T3 cells (3T3/vSrc) were obtained from O. Sartor (Tulane University, New Orleans, LA). Continuously growing adult fibroblast cell lines (see below) were cultured in DMEM with GlutaMAX supplemented with 10% (vol/vol) FBS and 100 U·mL^{-1} penicillin/100 U·mL^{-1} streptomycin in a humidified incubator with 5% CO_2 and 95% (vol/vol) O_2. Dasatinib was obtained from Bristol Myers Squibb. H_2O_2, ascorbic acid, oligomycin and FCCP and were obtained from Sigma. TRAP1 antibody was from BD Biosciences. Antibodies recognizing c-Src, phospho-Src (Tyr416), VDAC, and β-actin were from Cell Signaling Technology. Antibody recognizing GFP was from Santa Cruz Biotechnology. TOM70 and α-tubulin antibodies were obtained from Thermo Scientific and Calbiochem/Millipore, respectively.

Establishment of Immortalized Fibroblasts from Adult WT and TRAP1 KO Mice. Mice with a gene trap disruption of the *Trap1* gene were used to derive TRAP1-null cells. A piece of the ear of adult TRAP1$^{+/+}$ and TRAP1$^{-/-}$ mice was chopped and incubated overnight in a 3-cm dish with RPMI-1640 supplemented with 30% (vol/vol) NCS, 2 mM L-glutamine, 100 U·mL^{-1} penicillin/100 U·mL^{-1} streptomycin, and 1 mg/mL proteinase K. The next day, the resultant single cell suspension was centrifuged and transferred to fresh medium. After 1 wk, RPMI-1640 medium was replaced by DMEM with GlutaMAX, supplemented with 10% FBS and 100 U·mL^{-1} penicillin/100 U·mL^{-1} streptomycin. Cells were continuously passaged until they became spontaneously immortalized. Two independently derived TRAP$^{+/+}$ (WT) and TRAP$^{-/-}$ (KO) MAF cell lines were established. Where only one cell line of each type is examined, it is WT1 or KO1, respectively.

Plasmids, Gene Transfection, and RNAi. pEGFP-N1-human TRAP1-GFP was generously provided by D. Toft (Department of Biochemistry and Molecular Biology, Mayo Graduate School, Rochester, MN). Conventional molecular biological techniques were used to generate the pcDNA3-human TRAP1-Flag. Plasmid expressing WT c-Src was purchased from Upstate Biotechnology. Plasmids expressing mitochondrially targeted c-Src constructs were kind gifts of Y. Homma (Department of Biomolecular Science, Fukushima Medical University School of Medicine, Fukushima, Japan) (15). MAFs were transiently transfected with TRAP1-GFP or empty-GFP plasmid using an Amaxa Nucleofector (Lonza), according to the manufacturer's protocol. Otherwise, transient transfections were performed using X-tremeGENE 9 Transfection Reagent (Roche Applied Science). RNA interference was performed with siRNA specific for TRAP1 (ON-TARGETplus SMARTpool Mouse Trap1 or Human TRAP1, Thermo Scientific), or control nonspecific siRNA (MISSION siRNA Universal Negative Control; Sigma) using DharmaFECT Transfection Reagent (Thermo Scientific) according to the manufacturer's protocol.

Mitochondrial Respiration, Glycolysis, and Fatty Acid Oxidation. Mitochondrial respiration, aerobic glycolysis, and fatty acid oxidation were monitored in real time with the Seahorse Bioscience Extracellular Flux Analyzer (XF96; Seahorse Bioscience) by measuring the OCR (indicative of respiration) and ECAR (indicative of glycolysis). Further details are provided in *SI Methods*.

ATP Assay. ATP content of whole cell extracts was determined with a luminescent ATP detection kit (ATPlite; PerkinElmer) according to the manufacturer's instructions. Results were normalized to cell number.

ROS Determination. To measure total cellular ROS, cells were incubated with 10 μM chloromethyl-dichlorodihydrofluorescein diacetate (CM-H_2DCFDA; Life Technologies) for 1 h at 37 °C before being returned to prewarmed media without phenol red. After 1-h incubation, immunofluorescence was measured (VICTOR ^{3}V; PerkinElmer). Alternatively, mitochondrial ROS (superoxide) was assessed using the MitoSOX reagent (Life Technologies) and following manufacturer's instructions. Data were normalized to total protein.

Lipid Peroxidation. The end product of lipid peroxidation, malondialdhyde, was quantified using the TBARS assay kit from Cayman Chemical and following the manufacturer's instructions. Further details are provided in *SI Methods*.

In Vitro Cell Invasion Assay. HeLa cells (20×10^4) or HCT116 cells (10×10^4) 24 h after transfection, or mouse fibroblasts (10×10^4), were seeded in 24-well Matrigel-coated migration chambers (8-μm pores; BD Biosciences) in serum-free medium. The lower chamber was filled with complete medium containing 10% FBS. After incubation for 24 h (HeLa cells and fibroblasts) or 48 h (HCT116 cells), cells remaining in the upper chamber were removed with cotton swabs. The cells that migrated through the Matrigel and attached to the lower surface of the inserts were fixed and stained with Diff-Quik (Siemens). All experiments were conducted twice in duplicate for each condition.

Immunofluorescence Analysis. TRAP1 WT or KO MAFs were labeled with either MitoTracker Red (Life Technologies; mitochondrial mass) or JC-1 (Life Technologies; mitochondrial membrane potential), according to the manufacturer's instructions. Data were collected from 10,000 cells per condition by flow cytometry.

Immunohistochemistry. Immunostaining was performed on 5-μm paraffin-embedded tissue sections using TRAP1 antibody (TRAP1-6; Thermo Scientific). Briefly, the sections were rehydrated, treated in 0.3% hydrogen peroxide, and placed in a 550 W microwave oven for 15 min in 10 mM citrate buffer (pH 6.0). After incubation with 10% goat serum for 30 min, the sections were incubated with primary antibody overnight at 4 °C. The sec-

tions were incubated with horseradish peroxidase-labeled secondary antibody for 30 min at room temperature and color was developed with 3,3-diaminobenzidine. The sections were counterstained with hematoxylin. This study was approved by the Institutional Review Board of Tokyo Medical and Dental University and written informed consent was obtained from each patient whose tissue was evaluated.

Microarray Analysis. Two published microarray datasets (GDS) obtained from the National Center for Biotechnology Information Gene Expression Omnibus Web site (www.ncbi.nlm.nih.gov/geo) were used to interrogate TRAP1 gene expression in cervical cancer and normal cervix, and in several stages of bladder cancer. Wilcoxon signed-rank test was used to compare TRAP1 gene expression between groups. Boxes and whiskers represent interquartile range and range of all values, respectively.

Metabolomic Analysis. Sample preparation and analysis was carried out using established procedures (www.metabolon.com; Metabolon).

Statistics. Statistical analysis was performed using Microsoft Excel and JMP7.0 software. Unpaired Student t test, χ^2 test, or Wilcoxon rank-sum test was used to generate the P values for the datasets.

ACKNOWLEDGMENTS. We thank S. Felts and D. Toft (Department of Biochemistry and Molecular Biology, Mayo Graduate School) for TNF receptor-associated protein 1 plasmid and antibody, and Y. Homma (Department of Biomolecular Science, Fukushima Medical University School of Medicine) for mitochondrially targeted c-Src plasmids. This work was supported by funds from the Intramural Research Program of the National Cancer Institute, Center for Cancer Research. S.Y. received financial support for overseas study from The Waksman Foundation of Japan.

1. Picard D (2012) Preface to Hsp90. *Biochim Biophys Acta* 1823(3):605–606.
2. Trepel J, Mollapour M, Giaccone G, Neckers L (2010) Targeting the dynamic HSP90 complex in cancer. *Nat Rev Cancer* 10(8):537–549.
3. Leskovar A, Wegele H, Werbeck ND, Buchner J, Reinstein J (2008) The ATPase cycle of the mitochondrial Hsp90 analog Trap1. *J Biol Chem* 283(17):11677–11688.
4. Matassa DS, Amoroso MR, Maddalena F, Landriscina M, Esposito F (2012) New insights into TRAP1 pathway. *Am J Cancer Res* 2(2):235–248.
5. Montesano Gesualdi N, et al. (2007) Tumor necrosis factor-associated protein 1 (TRAP-1) protects cells from oxidative stress and apoptosis. *Stress* 10(4):342–350.
6. Im CN, Lee JS, Zheng Y, Seo JS (2007) Iron chelation study in a normal human hepatocyte cell line suggests that tumor necrosis factor receptor-associated protein 1 (TRAP1) regulates production of reactive oxygen species. *J Cell Biochem* 100(2): 474–486.
7. Hua G, Zhang Q, Fan Z (2007) Heat shock protein 75 (TRAP1) antagonizes reactive oxygen species generation and protects cells from granzyme M-mediated apoptosis. *J Biol Chem* 282(28):20553–20560.
8. Kang BH, et al. (2007) Regulation of tumor cell mitochondrial homeostasis by an organelle-specific Hsp90 chaperone network. *Cell* 131(2):257–270.
9. Xiang F, Huang YS, Shi XH, Zhang Q (2010) Mitochondrial chaperone tumour necrosis factor receptor-associated protein 1 protects cardiomyocytes from hypoxic injury by regulating mitochondrial permeability transition pore opening. *FEBS J* 277(8): 1929–1938.
10. Kang BH (2012) TRAP1 regulation of mitochondrial life or death decision in cancer cells and mitochondria-targeted TRAP1 inhibitors. *BMB Rep* 45(1):1–6.
11. Schulte TW, et al. (1999) Interaction of radicicol with members of the heat shock protein 90 family of molecular chaperones. *Mol Endocrinol* 13(9):1435–1448.
12. Whitesell L, Lindquist SL (2005) HSP90 and the chaperoning of cancer. *Nat Rev Cancer* 5(10):761–772.
13. Liu D, et al. (2010) Tumor necrosis factor receptor-associated protein 1(TRAP1) regulates genes involved in cell cycle and metastases. *Cancer Lett* 296(2):194–205.
14. Miyazaki T, Neff L, Tanaka S, Horne WC, Baron R (2003) Regulation of cytochrome *c* oxidase activity by c-Src in osteoclasts. *J Cell Biol* 160(5):709–718.
15. Ogura M, Yamaki J, Homma MK, Homma Y (2012) Mitochondrial c-Src regulates cell survival through phosphorylation of respiratory chain components. *Biochem J* 447(2): 281–289.
16. Mazumder R, Sasakawa T, Ochoa S (1963) Metabolism of propionic acid in animal tissues. X. Methylmalonyl co-enzyme A mutase holoenzyme. *J Biol Chem* 238:50–53.
17. Kaziro Y, Leone E, Ochoa S (1960) Biotin and propionyl carboxylase. *Proc Natl Acad Sci USA* 46(10):1319–1327.
18. Beck WS, Flavin M, Ochoa S (1957) Metabolism of propionic acid in animal tissues. III. Formation of succinate. *J Biol Chem* 229(2):997–1010.
19. Mingorance C, et al. (2012) Propionyl-L-carnitine corrects metabolic and cardiovascular alterations in diet-induced obese mice and improves liver respiratory chain activity. *PLoS ONE* 7(3):e34268.
20. Kemp RG, Gunasekera D (2002) Evolution of the allosteric ligand sites of mammalian phosphofructo-1-kinase. *Biochemistry* 41(30):9426–9430.
21. Li Y, Rivera D, Ru W, Gunasekera D, Kemp RG (1999) Identification of allosteric sites in rabbit phosphofructo-1-kinase. *Biochemistry* 38(49):16407–16412.
22. Jenkins CM, Yang J, Sims HF, Gross RW (2011) Reversible high affinity inhibition of phosphofructokinase-1 by acyl-CoA: A mechanism integrating glycolytic flux with lipid metabolism. *J Biol Chem* 286(14):11937–11950.
23. Schaffer SW, Azuma J, Mozaffari M (2009) Role of antioxidant activity of taurine in diabetes. *Can J Physiol Pharmacol* 87(2):91–99.
24. Messina SA, Dawson R, Jr. (2000) Attenuation of oxidative damage to DNA by taurine and taurine analogs. *Adv Exp Med Biol* 483:355–367.
25. Guérin P, El Mouatassim S, Ménézo Y (2001) Oxidative stress and protection against reactive oxygen species in the pre-implantation embryo and its surroundings. *Hum Reprod Update* 7(2):175–189.
26. Duprè S, et al. (1998) Hypotaurine protection on cell damage by H2O2 and on protein oxidation by Cu+2 and H2O2. *Adv Exp Med Biol* 442:17–23.
27. Al-Majed AA, et al. (2006) Carnitine esters prevent oxidative stress damage and energy depletion following transient forebrain ischaemia in the rat hippocampus. *Clin Exp Pharmacol Physiol* 33(8):725–733.
28. Calò LA, et al. (2006) Antioxidant effect of L-carnitine and its short chain esters: Relevance for the protection from oxidative stress related cardiovascular damage. *Int J Cardiol* 107(1):54–60.
29. Gómez-Amores L, Mate A, Revilla E, Santa-María C, Vázquez CM (2006) Antioxidant activity of propionyl-L-carnitine in liver and heart of spontaneously hypertensive rats. *Life Sci* 78(17):1945–1952.
30. Salvi M, et al. (2002) Characterization and location of Src-dependent tyrosine phosphorylation in rat brain mitochondria. *Biochim Biophys Acta* 1589(2):181–195.
31. Augereau O, et al. (2005) Identification of tyrosine-phosphorylated proteins of the mitochondrial oxidative phosphorylation machinery. *Cell Mol Life Sci* 62(13):1478–1488.
32. Livigni A, et al. (2006) Mitochondrial AKAP121 links cAMP and src signaling to oxidative metabolism. *Mol Biol Cell* 17(1):263–271.
33. Tibaldi E, et al. (2008) Src-Tyrosine kinases are major agents in mitochondrial tyrosine phosphorylation. *J Cell Biochem* 104(3):840–849.
34. Martin J (1997) Molecular chaperones and mitochondrial protein folding. *J Bioenerg Biomembr* 29(1):35–43.
35. Tochhawng L, Deng S, Pervaiz S, Yap CT (2012) Redox regulation of cancer cell migration and invasion. *Mitochondrion* S1567-7249(12)00203–00206.
36. Ray PD, Huang BW, Tsuji Y (2012) Reactive oxygen species (ROS) homeostasis and redox regulation in cellular signaling. *Cell Signal* 24(5):981–990.
37. Costantino E, et al. (2009) TRAP1, a novel mitochondrial chaperone responsible for multi-drug resistance and protection from apoptotis in human colorectal carcinoma cells. *Cancer Lett* 279(1):39–46.
38. Fang HY, et al. (2009) Hypoxia-inducible factors 1 and 2 are important transcriptional effectors in primary macrophages experiencing hypoxia. *Blood* 114(4):844–859.
39. Ramasamy A (2009) Increasing statistical power and generalizability in genomics microarray research. PhD thesis (Univ of Oxford, Oxford).
40. Felts SJ, et al. (2000) The hsp90-related protein TRAP1 is a mitochondrial protein with distinct functional properties. *J Biol Chem* 275(5):3305–3312.
41. Altieri DC (2011) Mitochondrial compartmentalized protein folding and tumor cell survival. *Oncotarget* 2(4):347–351.
42. Kang BH, et al. (2011) Targeted inhibition of mitochondrial Hsp90 suppresses localised and metastatic prostate cancer growth in a genetic mouse model of disease. *Br J Cancer* 104(4):629–634.
43. Moreno-Sánchez R, Rodríguez-Enríquez S, Marín-Hernández A, Saavedra E (2007) Energy metabolism in tumor cells. *FEBS J* 274(6):1393–1418.
44. Chae YC, et al. (2012) Control of tumor bioenergetics and survival stress signaling by mitochondrial HSP90s. *Cancer Cell* 22(3):331–344.
45. Liu Y (2006) Fatty acid oxidation is a dominant bioenergetic pathway in prostate cancer. *Prostate Cancer Prostatic Dis* 9(3):230–234.
46. Barbi de Moura M, et al. (2012) Mitochondrial respiration—An important therapeutic target in melanoma. *PLoS ONE* 7(8):e40690.
47. Xu Y, Singer MA, Lindquist S (1999) Maturation of the tyrosine kinase c-src as a kinase and as a substrate depends on the molecular chaperone Hsp90. *Proc Natl Acad Sci USA* 96(1):109–114.
48. Koga F, et al. (2006) Hsp90 inhibition transiently activates Src kinase and promotes Src-dependent Akt and Erk activation. *Proc Natl Acad Sci USA* 103(30):11318–11322.
49. Yano A, et al. (2008) Inhibition of Hsp90 activates osteoclast c-Src signaling and promotes growth of prostate carcinoma cells in bone. *Proc Natl Acad Sci USA* 105(40): 15541–15546.
50. Kim LC, Song L, Haura EB (2009) Src kinases as therapeutic targets for cancer. *Nat Rev Clin Oncol* 6(10):587–595.
51. Moreno-Sánchez R, Rodríguez-Enríquez S, Saavedra E, Marín-Hernández A, Gallardo-Pérez JC (2009) The bioenergetics of cancer: Is glycolysis the main ATP supplier in all tumor cells? *Biofactors* 35(2):209–225.
52. Caro P, et al. (2012) Metabolic signatures uncover distinct targets in molecular subsets of diffuse large B cell lymphoma. *Cancer Cell* 22(4):547–560.
53. Bonuccelli G, et al. (2010) Ketones and lactate "fuel" tumor growth and metastasis: Evidence that epithelial cancer cells use oxidative mitochondrial metabolism. *Cell Cycle* 9(17):3506–3514.
54. Nakajima EC, Van Houten B (2012) Metabolic symbiosis in cancer: Refocusing the Warburg lens. *Mol Carcinog*, 10.1002/mc.21863.
55. DeBerardinis RJ, Lum JJ, Hatzivassiliou G, Thompson CB (2008) The biology of cancer: Metabolic reprogramming fuels cell growth and proliferation. *Cell Metab* 7(1):11–20.
56. Mullen AR, DeBerardinis RJ (2012) Genetically-defined metabolic reprogramming in cancer. *Trends Endocrinol Metab* 23(11):552–559.